INORGANIC COMPOUNDS

Acta Cryst. (1998). C**54**, 2–5

$Pb_2Fe_2Ge_2O_9$, the Germanate Analogue of the Silicate Mineral Melanotekite

JACQUES BARBIER AND DAVID LÉVY

Department of Chemistry, McMaster University, Hamilton, Ontario L8S 4M1, Canada. E-mail: barbier@mcmaster.ca

(Received 19 May 1997; accepted 26 September 1997)

Abstract

The structure of dilead(II) diiron(III) digermanium(IV) oxide, with a minor (2Fe/Mg+Ge) substitution arising from the growth conditions, has been determined using flux-grown single crystals. Interesting features of the structure include an unsymmetrical splitting of the Pb site and a strong anisotropy of the bridging O atom of the Ge_2O_7 group, both of which also occur in the structure of the silicate mineral melanotekite, $Pb_2Fe_2Si_2O_9$. These structural features can be associated with the stereoactivity of the Pb^{2+} lone pairs, which is found to be less pronounced in the germanate than in the silicate structure.

Comment

The $Pb_2Fe_2Ge_2O_9$ compound has previously been synthesized in microcrystalline form and has been identified by powder X-ray diffraction as an analogue of the silicate mineral melanotekite, $Pb_2Fe_2Si_2O_9$ (Gabelica-Robert & Tarte, 1979). In fact, the crystal structure of the silicate mineral itself was only recently solved in the correct space group, *Pbcn*, for a $Pb_2(Mn,Fe)_2Si_2O_9$ mixed composition along the kentrolite–melanotekite series (Moore *et al.*, 1991), following an early attempt in the $C222_1$ space group (Gabrielson, 1962). The structure determination in *Pbcn* revealed a splitting of the Pb site in the $Pb_2(Mn,Fe)_2Si_2O_9$ structure, which was attributed to the stereoactive lone pair of the Pb^{2+} cation (Moore *et al.*, 1991). Similar splitting of Pb sites has also been reported in the structures of other Pb^{2+}-containing compounds, such as $PbFe_{12}O_{19}$ (Moore *et al.*, 1989) and $PbAl_2Si_2O_8$ (Benna *et al.*, 1996). In view of the difficulties encountered during the structure refinement of the melanotekite mineral [*i.e.* diffuse streaking in precession photographs, violations of space-group absences, non-positive definite displacement parameter for one O atom (Moore *et al.*, 1991)], and because good-quality crystals of the $Pb_2Fe_2Ge_2O_9$ compound were available, it was decided to carry out the structure determination of the germanate analogue for comparison purposes.

The $Pb_2Fe_2Ge_2O_9$ structure is shown in Fig. 1 projected onto the (100) plane. The structure contains zigzag rows of edge-sharing FeO_6 octahedra running along the [001] direction, linked *via* corner-sharing with Ge_2O_7 groups. The Pb atoms occupy irregular sites between the octahedral rows. The overall composition of $Pb_2Fe_{1.78}Ge_{2.11}Mg_{0.11}O_9$ (based on refined occupancies and microprobe analysis) is achieved *via* a double substitution ($2Fe^{3+} = Mg^{2+} + Ge^{4+}$) taking place on the octahedral sites: the larger *M*2 site [$\langle M2—O\rangle$ = 2.033 (3) Å, V = 10.96 Å^3] contains 89% Fe plus 11% Mg, while the slightly smaller *M*1 site [$\langle M1—O\rangle$ = 2.005 (3) Å, V = 10.60 Å^3] contains 89% Fe plus 11% Ge. The presence of Ge^{4+} on the smaller *M*1 site is also consistent with the greater regularity of that site on a centre of symmetry and with an angle variance of 30.2 (Robinson *et al.*, 1971), as compared to the *M*2 site on a twofold axis with an angle variance of 46.8. The greater distortion of the *M*2 site can also be linked to its asymmetric mode of corner-sharing with the Ge_2O_7 groups (*cf.* Fig. 1): the two O1 atoms of the $M2O_6$ octahedron are shared with two distinct Ge_2O_7 groups [yielding an O1···O1 edge length of 2.793 (5) Å], whereas the two O3 atoms are shared with the same Ge_2O_7 group [yielding a longer O3···O3 edge length of 3.006 (5) Å].

In the structure of the $Pb_2(Mn,Fe)_2Si_2O_9$ mineral, an additional cause of octahedral distortion corresponds to

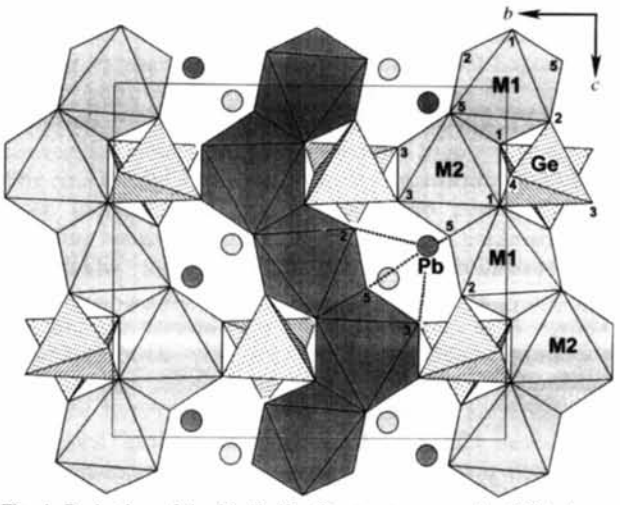

Fig. 1. Projection of the $Pb_2Fe_2Ge_2O_9$ structure onto the (100) plane. The edge-sharing FeO_6 octahedra form zigzag rows running parallel to the **c** direction which are linked *via* corner-sharing with Ge_2O_7 groups. Light- and dark-shaded octahedra are at heights $x = \frac{1}{2}$ and 0, respectively. The circles represent Pb atoms occupying irregular four-coordinate sites in channels parallel to the **a** direction [only one position (Pb1) of the split Pb site is shown]. *M*1 is Fe^{3+}/Ge^{4+} and *M*2 is Fe^{3+}/Mg^{2+}. The numbers 1–5 correspond to the O1–O5 atoms.

the presence of Jahn–Teller Mn^{3+} ($3d^4$) cations on the $M1$ and $M2$ sites. A random distribution of (68% Mn^{3+}, 32% Fe^{3+}) was necessarily assumed during the structure determination by X-ray diffraction (Moore *et al.*, 1991) and the strong opposite distortions of the $M1O_6$ octahedron [$M1$—O = 1.923 (8) (×2), 1.977 (8) (×2), 2.137 (10) Å (×2)] and the $M2O_6$ octahedron [$M2$—O = 1.882 (8) (×2), 2.091 (9) (×2), 2.108 (9) Å (×2)] were both attributed to their high Mn^{3+} content. The present study shows, however, that similar octahedral distortions are also observed in the $Pb_2Fe_2Ge_2O_9$ structure (albeit with reduced magnitude; *cf.* Table 2) in spite of the absence of any Jahn–Teller ion. This clearly indicates that the bonding topology of the melanotekite structure type together with the stereoactivity of the Pb^{2+} lone pairs (see below) are also important (and possibly the dominant) factors governing the structural distortions.

Except for the Pb2 site, which has a very low occupancy, the largest anisotropy in displacement parameters in the $Pb_2Fe_2Ge_2O_9$ structure is observed for the O4 atom [U_{11} = 0.0083 (16), U_{22} = 0.0098 (14), U_{33} = 0.0391 (26) Å^2], which occupies the bridging position in the Ge_2O_7 groups. A similarly large anisotropy along the **c** direction also occurs for the equivalent O-atom site in the melanotekite structure (Moore *et al.*, 1991). The O4 atom is bonded to two Ge atoms only (*cf.* Fig. 1) and the Ge—O4 bonds are, as expected, the longest tetrahedral bonds [1.762 (2) Å]. Nevertheless, the bond valences around the O4 atom sum to 1.93, which indicates a proper bonding environment; the latter, therefore, does not explain the strong O4 anisotropy. This anisotropy, however, can be associated with the stereoactivity of the lone electron pairs carried by the Pb^{2+} cations; as shown in Fig. 2, these cations occupy the apices of very distorted square pyramids and their lone pairs are expected to point away from the bonded O2, O3 and O5 (×2) atoms and towards the O4 atom of the nearby Ge_2O_7 group. The O4 atom is positioned on a twofold axis at (0, y, $\frac{1}{4}$) and is, consequently, interacting with the lone pair of two equidistant Pb^{2+} cations [O4···Pb1 = 3.161 (3) Å]. The major component of its anisotropic displacement (in the **c** direction) is nearly parallel to the line joining the two Pb^{2+} sites (see Fig. 2) and is probably a result of the interactions with the Pb^{2+} lone pairs. In that respect, it is noteworthy that the O4 anisotropy in the melanotekite structure [U_{11} = 0.0059 (51), U_{22} = 0.0109 (57), U_{33} = 0.0546 (100) Å^2 (Moore *et al.*, 1991)] is significantly more pronounced than in the germanate structure. The difference is likely due to the smaller unit-cell volume of the silicate (764.2 *versus* 809.6 Å^3), resulting in greater stereoactivity of the Pb^{2+} lone pairs. Indeed, in spite of the smaller melanotekite unit cell, the O4···Pb1 distance is actually longer in the silicate structure than in the germanate structure [3.216 (10) *versus* 3.161 (3) Å], and this is consistent with stronger interactions between the Pb^{2+} lone pairs and the O4 atom. This increased lone-pair stereoactivity also correlates well with the degree of Pb-site splitting, which is found to be larger in the silicate than in the germanate structure (Pb1/Pb2 = 73/27 and 91/9, respectively), and with the Pb1–Pb2 separation, which is also larger in the former [0.558 (16) *versus* 0.464 (7) Å].

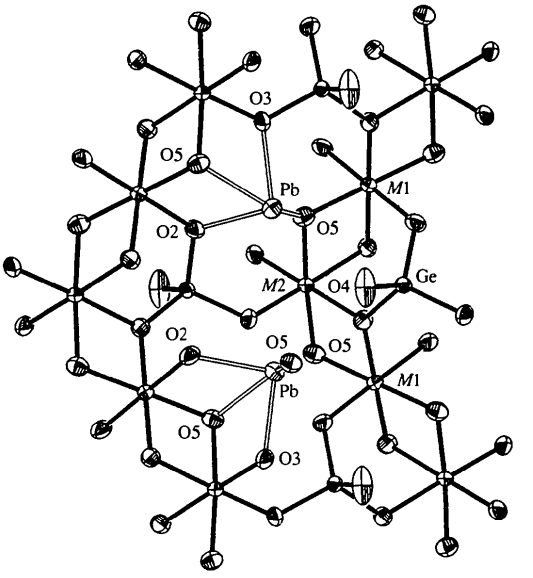

Fig. 2. Detail of the $Pb_2Fe_2Ge_2O_9$ structure viewed near the [100] direction emphasizing the coordination of the Pb1 site and the anisotropic displacements of all atoms (ellipsoids are drawn for 90% probability). $M1$ is Fe^{3+}/Ge^{4+} and $M2$ is Fe^{3+}/Mg^{2+}. The Pb^{2+} cations (at x = 0.06 and 0.94) are at the apices of very distorted square pyramids and are equidistant (3.16 Å) from the bridging O4 atom (at x = 0) of a Ge_2O_7 group. The Pb^{2+} lone pairs (not drawn) are both pointing towards the O4 atom and these interactions cause the strong O4 anisotropy.

Experimental

Single crystals of the $Pb_2(Fe,Mg,Ge)_2O_9$ compound were obtained during an attempt to grow crystals of another germanate compound, namely $MgFe_2Ge_2O_8$, by the flux method. A mixture of 4.8 g of $MgFe_2Ge_2O_8$ (pre-reacted at 1398 K) plus 2.45 g of GeO_2 was dissolved in a PbO–B_2O_3 flux (2.40 g PbO + 0.85 g B_2O_3). The melt was kept at 1323 K for 5 h, slowly cooled to 1073 K at 1.8 K h^{-1} and finally quenched in air. After soaking in hot water overnight, the recovered products included a dark red–brown glass, dark brown plate-like crystals of $Pb_2Fe_2Ge_2O_9$ and light yellow–brown thin plates of an $MgGeO_3$–Fe_2O_3 pyroxene solid solution. The microprobe analysis of the dark brown crystals indicated that they contained a small amount of MgO (approximately 0.5 wt%), yielding an average composition of $Pb_{2.01}Fe_{1.82}Ge_{2.07}Mg_{0.11}O_{8.99}$ (average of three analyses on three crystals). This composition is in good agreement with that derived from the refinement of site occupancies and corresponds to the double substitution $2Fe^{3+} = Mg^{2+} + Ge^{4+}$ (*cf. Comment*).

Crystal data

$Pb_2Fe_{1.78}Ge_{2.11}Mg_{0.11}O_9$ — Ag $K\alpha$ radiation
M_r = 813.67 — λ = 0.56086 Å

Orthorhombic
Pbcn
a = 7.1486 (14) Å
b = 11.163 (2) Å
c = 10.145 (2) Å
V = 809.6 (3) Å^3
Z = 4
D_x = 6.675 Mg m^{-3}
D_m not measured

Cell parameters from 25 reflections
θ = 7.35–14.74°
μ = 28.331 mm^{-1}
T = 293 (2) K
($\bar{1}$10) plate
0.3 × 0.15 × 0.025 mm
Brown

Data collection

Siemens *R3m/V* diffractometer
$\theta/2\theta$ scans
Absorption correction: Gaussian (*XPREP* in *SHELXL*93; Sheldrick, 1993)
T_{min} = 0.036, T_{max} = 0.495
4579 measured reflections
3667 independent reflections

2341 reflections with $F > 4\sigma(F)$
R_{int} = 0.052
θ_{max} = 35.10°
$h = -1 \rightarrow 14$
$k = -1 \rightarrow 22$
$l = -1 \rightarrow 20$
3 standard reflections
every 100 reflections
intensity decay: none

Refinement

Refinement on F^2
$R[F^2 > 2\sigma(F^2)]$ = 0.032
$wR(F^2)$ = 0.063
S = 0.868
3665 reflections
81 parameters
$w = 1/[\sigma^2(F_o^2) + (0.0258P)^2]$

$(\Delta/\sigma)_{max}$ = 0.001
$\Delta\rho_{max}$ = 2.02 e Å^{-3}
$\Delta\rho_{min}$ = −4.84 e Å^{-3}
Extinction correction: none
Scattering factors from *International Tables for Crystallography* (Vol. C)

Table 1. *Fractional atomic coordinates and equivalent isotropic displacement parameters (Å^2)*

$U_{eq} = (1/3)\Sigma_i\Sigma_j U^{ij} a_i^* a_j^* \mathbf{a}_i.\mathbf{a}_j$.

	x	y	z	U_{eq}
Pb1†	0.94026 (3)	0.19986 (3)	0.04620 (3)	0.01220 (4)
Pb2‡	1.0051 (11)	0.2012 (4)	0.0445 (4)	0.0536 (14)
Ge	0.21729 (5)	−0.08545 (3)	0.24996 (4)	0.00676 (6)
*M*1§	0	1/2	0	0.00753 (12)
*M*2¶	0	−0.34909 (6)	1/4	0.0071 (2)
O1	0.3503 (4)	0.0149 (2)	0.1615 (3)	0.0099 (4)
O2	0.3121 (5)	−0.1132 (2)	0.4049 (3)	0.0131 (5)
O3	0.1791 (4)	−0.2232 (2)	0.1725 (3)	0.0111 (5)
O4	0	−0.0109 (3)	1/4	0.0191 (9)
O5	0.1191 (4)	0.3561 (2)	−0.0743 (3)	0.0103 (4)

† Site occupancy = 0.91 (1). ‡ Site occupancy = 0.09 (1). § Site occupancy = 0.893 (5) Fe, 0.107 (5) Ge. ¶ Site occupancy = 0.893 (5) Fe, 0.107 (5) Mg.

Table 2. *Selected geometric parameters (Å, °)*

Pb1—O2^{i}	2.333 (3)	Ge—O4	1.762 (2)
Pb1—O3^{ii}	2.391 (3)	*M*1—O1^{viii}	1.964 (3)
Pb1—O5^{iii}	2.396 (3)	*M*1—O1^{vii}	1.964 (3)
Pb1—O5^{iv}	2.484 (3)	*M*1—O5	1.969 (3)
Pb1···O4^{iv}	3.161 (3)	*M*1—O5^{ix}	1.969 (3)
Pb1—O2^{v}	3.171 (3)	*M*1—O2^{x}	2.082 (3)
Pb1—O3^{vi}	3.127 (3)	*M*1—O2^{xi}	2.082 (3)
Pb1–Pb2	0.464 (7)	*M*2—O5^{xii}	1.977 (3)
Pb1—Pb2^{vii}	3.427 (7)	*M*2—O5^{xiii}	1.977 (3)
Pb2—O5^{iv}	2.259 (5)	*M*2—O3	2.058 (3)
Pb2—O2^{i}	2.542 (7)	*M*2—O3^{xiv}	2.058 (3)
Pb2—O3^{ii}	2.577 (7)	*M*2—O1^{xv}	2.063 (3)
Pb2—O3^{vi}	2.737 (8)	*M*2—O1^{xvi}	2.063 (3)
Pb2···O4^{iv}	3.155 (3)	O4—Ge	1.762 (2)
Pb2—O2^{v}	2.791 (3)	O4—Ge^{xvii}	1.762 (2)
Pb2—O3^{vi}	2.737 (3)	O4···Pb1^{xviii}	3.161 (3)
Ge—O1	1.722 (3)	O4···Pb1^{xix}	3.161 (3)
Ge—O2	1.739 (3)	O4···Pb2^{xviii}	3.155 (3)
Ge—O3	1.748 (3)	O4···Pb2^{xix}	3.155 (3)
O1—Ge—O2	111.81 (14)	O5^{ix}—*M*1—O2^{x}	87.77 (12)
O1—Ge—O3	115.09 (13)	O2^{x}—*M*1—O2^{xi}	180.0
O2—Ge—O3	108.10 (13)	O5^{xii}—*M*2—O5^{xiii}	175.5 (2)
O1—Ge—O4	100.35 (13)	O5^{xii}—*M*2—O3	95.94 (12)
O2—Ge—O4	115.30 (11)	O5^{xiii}—*M*2—O3	87.14 (12)
O3—Ge—O4	106.14 (14)	O5^{xiii}—*M*2—O3^{xiv}	95.94 (12)
O1^{viii}—*M*1—O1^{vii}	180.0	O3—*M*2—O3^{xiv}	93.8 (2)
O1^{viii}—*M*1—O5	98.80 (11)	O5^{xii}—*M*2—O1^{xv}	78.60 (11)
O1^{vii}—*M*1—O5	81.20 (11)	O5^{xiii}—*M*2—O1^{xv}	98.04 (11)
O5—*M*1—O5^{ix}	180.0	O3—*M*2—O1^{xv}	172.68 (11)
O1^{viii}—*M*1—O2^{x}	89.07 (12)	O3^{xiv}—*M*2—O1^{xv}	90.77 (11)
O1^{vii}—*M*1—O2^{x}	90.93 (12)	O1^{xv}—*M*2—O1^{xvi}	85.2 (2)
O5—*M*1—O2^{x}	92.23 (12)		

Symmetry codes: (i) $\frac{1}{2}+x, \frac{1}{2}+y, \frac{1}{2}-z$; (ii) $1-x, -y, -z$; (iii) $\frac{1}{2}+x, \frac{1}{2}-y, -z$; (iv) $1+x, y, z$; (v) $1+x, -y, z-\frac{1}{2}$; (vi) $\frac{3}{2}-x, \frac{1}{2}+y, z$; (vii) $x-\frac{1}{2}, \frac{1}{2}-y, -z$; (viii) $\frac{1}{2}-x, \frac{1}{2}+y, z$; (ix) $-x, 1-y, -z$; (x) $\frac{1}{2}-x, \frac{1}{2}-y, z-\frac{1}{2}$; (xi) $x-\frac{1}{2}, \frac{1}{2}+y, \frac{1}{2}-z$; (xii) $x, -y, \frac{1}{2}+z$; (xiii) $-x, -y, -z$; (xiv) $-x, y, \frac{1}{2}-z$; (xv) $x-\frac{1}{2}, y-\frac{1}{2}, \frac{1}{2}-z$; (xvi) $\frac{1}{2}-x, y-\frac{1}{2}, z$; (xvii) $-x, y, \frac{1}{2}-z$; (xviii) $x-1, y, z$; (xix) $1-x, y, \frac{1}{2}-z$.

A $Pb_2Fe_2Ge_2O_9$ single crystal suitable for data collection was selected by examination with an optical microscope and a precession camera. The extinctions observed on the [*h*0*l*] and [0*kl*] precession photographs were consistent with the *Pbcn* space group previously determined for the melanotekite mineral, $Pb_2(Fe,Mn)_2Si_2O_9$ (Moore *et al.*, 1991). However, unlike observations reported for the silicate mineral, no diffuse streaks were observed on the precession films.

The crystal used for the data collection was a thin plate approximated as a parallelepiped bounded by ±(0,0,1), ±(1,2,0) and ±($\bar{1}$,1,0) faces with corresponding dimensions of 0.300, 0.150 and 0.025 mm. The raw intensity data were corrected for absorption according to the crystal shape using the *XPREP* routine of the *SHELXL*93 package (Sheldrick, 1993). The structure was then determined by a combination of direct methods and Fourier syntheses (Sheldrick, 1990*a*, 1993).

During the refinement, a large residual electron density was found near the Pb site, which was then further refined as a split Pb1–Pb2 site, as had been performed for the $Pb_2(Fe,Mn)_2Si_2O_9$ structure (Moore *et al.*, 1991). The occupancies of the Pb1 and Pb2 sites were then constrained to sum to 1.0 but their displacement parameters were left unconstrained. The rather large final U_{eq} of the Pb2 site reflects its very low occupancy (9.1%). Attempts to refine the structure with a single strongly anisotropic Pb site were unsuccessful.

The small amount of MgO, the excess of GeO_2 and the deficiency in Fe_2O_3 determined by the electron microprobe analysis have been taken into account by introducing a double substitution ($2Fe^{3+} = Mg^{2+} + Ge^{4+}$) on the octahedral sites of the structure: Mg^{2+} was assumed to replace Fe^{3+} in the slightly larger *M*2 site, which also had a larger U_{eq} parameter initially, while Ge^{4+} was introduced on the smaller *M*1 site. The refinement of constrained occupancies yielded a 10.7% (±0.5%) substitution on both sites, corresponding to an overall composition of $Pb_2Fe_{1.78}Ge_{2.11}Mg_{0.11}O_9$, in good agreement with the microprobe analysis.

In the final cycles of refinement, the 004 and 0,0,10 reflections were omitted because of their abnormally large ($F_o^2 - F_c^2$)/s.u. ratios of 20.2 and 10.0, respectively. In the final electron density difference map, both the minimum (−4.9 e Å^{-3}) and maximum (2.0 e Å^{-3}) occur at approximately 0.5 Å away from the Pb1 site.

Data collection: *XSCANS* (Siemens, 1991). Cell refinement: *XSCANS*. Data reduction: *XSCANS*. Program(s) used to solve structure: *SHELXS*86 (Sheldrick, 1990*a*). Program(s) used to refine structure: *SHELXL*93 (Sheldrick, 1993). Molecular graphics: *SHELXTL XP* (Sheldrick, 1990*b*). Software used to prepare material for publication: *SHELXL*93.

The diffraction data were collected by Dr J. Britten (Department of Chemistry, McMaster University) and the microprobe analysis was carried out by Dr C. Cermignani (Department of Earth Sciences, University of Toronto). The work was supported by a research grant to JB from the Canadian Natural Sciences and Engineering Research Council.

Supplementary data for this paper are available from the IUCr electronic archives (Reference: TA1174). Services for accessing these data are described at the back of the journal.

References

Benna, P., Tribaudino, M. & Bruno, E. (1996). *Am. Mineral.* **81**, 1337–1343.
Gabelica-Robert, M. & Tarte, P. (1979). *J. Solid State Chem.* **27**, 179–190.
Gabrielson, O. (1962). *Ark. Mineral. Geol.* **3**, 141–151.
Moore, P. B., Sen Gupta, P. K. & Le Page, Y. (1989). *Am. Mineral.* **74**, 1186–1194.
Moore, P. B., Sen Gupta, P. K., Shen, J. & Schlemper, E. O. (1991). *Am. Mineral.* **76**, 1389–1399.
Robinson, K., Gibbs, G. V. & Ribbe, P. H. (1971). *Science*, **172**, 567–570.
Sheldrick, G. M. (1990*a*). *Acta Cryst.* A**46**, 467–473.
Sheldrick, G. M. (1990*b*). *SHELXTL/PC User's Manual*. Siemens Analytical X-ray Instruments Inc., Madison, Wisconsin, USA.
Sheldrick, G. M. (1993). *SHELXL*93. *Program for the Refinement of Crystal Structures*. University of Göttingen, Germany.
Siemens (1991). *XSCANS Users Manual*. Siemens Analytical X-ray Instruments Inc., Madison, Wisconsin, USA.

Acta Cryst. (1998). C**54**, 5–7

Ga_3PO_7

SOPHIE BOUDIN AND KWANG-HWA LII

Institute of Chemistry, Academia Sinica, Taipei, Taiwan.
E-mail: lii@chem.sinica.edu.tw

(*Received 17 March 1997; accepted 30 July 1997*)

Abstract

Trigallium phosphorus heptaoxide was synthesized by high-pressure hydrothermal synthesis. Its structure comprises PO_4 tetrahedra and GaO_5 trigonal bipyramids connected by edges to form Ga_3O_{10} clusters. It is isotypic with Fe_3PO_7 and is the third known compound in the Ga–P–O system.

Comment

Gallium phosphates are rare in the literature. In the Ga–P–O system, only two forms of $GaPO_4$ have been observed previously: the cristobalite (Mooney, 1956) and the α-quartz structure type (Litvin *et al.*, 1987). The structure of the latter has been widely studied under different pressures and temperatures (Sowa, 1994; Nakae *et al.*, 1995) as its compressibility properties are similar to those of the SiO_2 quartz phases. However, no new forms have been observed. By using high-pressure hydrothermal synthesis, we have isolated a third gallium phosphate, Ga_3PO_7, isotypic with the Fe_3PO_7 iron phosphate (Modaressi *et al.*, 1983) and report its structure here.

The Ga_3PO_7 structure (Figs. 1 and 2) contains Ga_3O_{10} clusters of three GaO_5 trigonal bipyramids. Within a cluster, each GaO_5 bipyramid shares two adjacent edges with two others. In this compact structure, each cluster shares six corners with six Ga–O clusters and four corners with four PO_4 tetrahedra. A comparison with the iron analogue shows that the gallium phosphate has smaller cell parameters, in agreement with the smaller size of the Ga^{3+} ion. Moreover, the Ga^{3+}—O distances, ranging from 1.863 (4) to 2.140 (3) Å, are

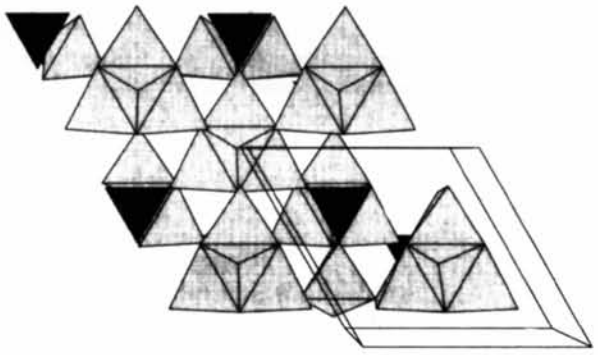

Fig. 1. Perspective view of the Ga_3PO_7 structure projected along the *c* axis with the *a* axis horizontal and the *b* axis close to vertical. The GaO_5 and PO_4 polyhedra are represented as light and medium gray, respectively.

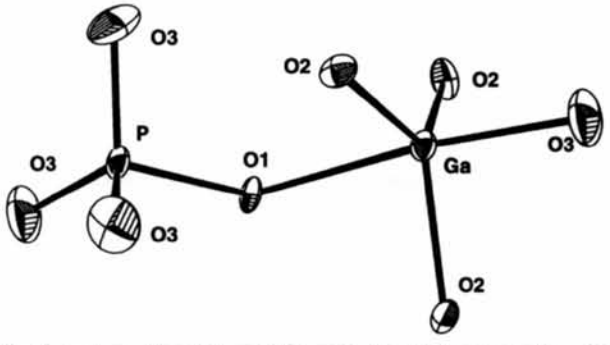

Fig. 2. A view of the GaO_5 and PO_4 units. The displacement ellipsoids are plotted at the 90% probability level.